

Achromatic Linear Polarization Switch for Visible and Near Infrared Radiation Based on Dual-Frequency Twisted Nematic Cell

Andrii B. Golovin, Oleg P. Pishnyak, Sergij V. Shiyanovskii, and Oleg D. Lavrentovich
 Liquid Crystal Institute and Chemical Physics Interdisciplinary Program,
 Kent State University, Kent, Ohio 44242-0001, USA
 Email: odl@lci.kent.edu, Fax: (330)672-2796, Phone: (330)672-4844

We developed a broad band achromatic linear polarization switch for visible and near infrared radiation. The achromatic switch is based on a twisted nematic cell filled with a dual-frequency nematic material. The switch is capable of fast switching linearly polarized light between two orthogonal directions with a switching time in the millisecond range.

Keywords: achromatic linear polarization rotator, visible and near infrared radiation, dual-frequency twisted nematic cell.

1. INTRODUCTION

The switchable polarization rotators are of prime importance in many modern optical applications, such as displays, spatial light modulators, and beam deflectors. Such a rotator can be designed with a half-wave electrically controlled nematic cell with antiparallel alignment at the two boundary plates. However, this rotator can operate only in a narrow spectral band where the half-wave condition is satisfied. A rotator comprised of multiple liquid crystal (LC) cells can provide a broader operational spectral region [1, 2]. A twisted nematic (TN) cell alone can provide the achromatic polarization rotation controlled by an applied electric field [3]. An ‘ideal’ achromatic rotation for a broad optical range with a high contrast (a small induced ellipticity) might be achieved when the cell thickness d , light wavelength λ and the nematic birefringence Δn satisfy the Mauguin condition $d \gg \lambda/2\Delta n$ [4, 5]. Unfortunately, a large d needed to satisfy this condition causes a long switching time of the nematic device, $\tau\alpha d^2$, see, for example Ref. [6]. Several approaches have been suggested to use rather thin TN cells for polarization rotation [7-11], however their dynamics have not been explored. Recently we have shown that by using dual-frequency nematics one can significantly speed up a switching of rather thick nematic cells with antiparallel alignment and large “pretilt” angle [12-14]. In this work, we present the first results on the dynamics of dual-frequency TN cells and evaluate their performance as polarization rotators. We demonstrated the operation of electrically switchable thick TN cells as achromatic linear polarization rotators for the wavelength range between 0.4 μ m and 2.7 μ m with fast switching within 10 ms.

2. OPTICAL DESIGN

It is well known that the wave equation for light propagation in helical structure along the helical axis has an exact solution [15]. Analysis of this solution shows that a relatively thick TN cell rotates the linearly polarized light achromatically: The vector of electric field follows the twisted director structure of the TN cell. This wave-guiding effect occurs if the thickness of the TN cell d satisfies the Mauguin condition written as $u \gg 1$, where $u = \pi d \Delta n / \lambda \Theta$ is the Mauguin parameter, and Θ is the angle of total twist [4, 16].

To analyze the Mauguin condition quantitatively, one can calculate the transmittance T of the TN cell placed between a polarizer oriented along the director at the entrance plate and an analyzer oriented perpendicularly to the director at the exit plate [5]:

$$T = \frac{\sin^2(\Theta\sqrt{1+u^2})}{1+u^2}. \quad (1)$$

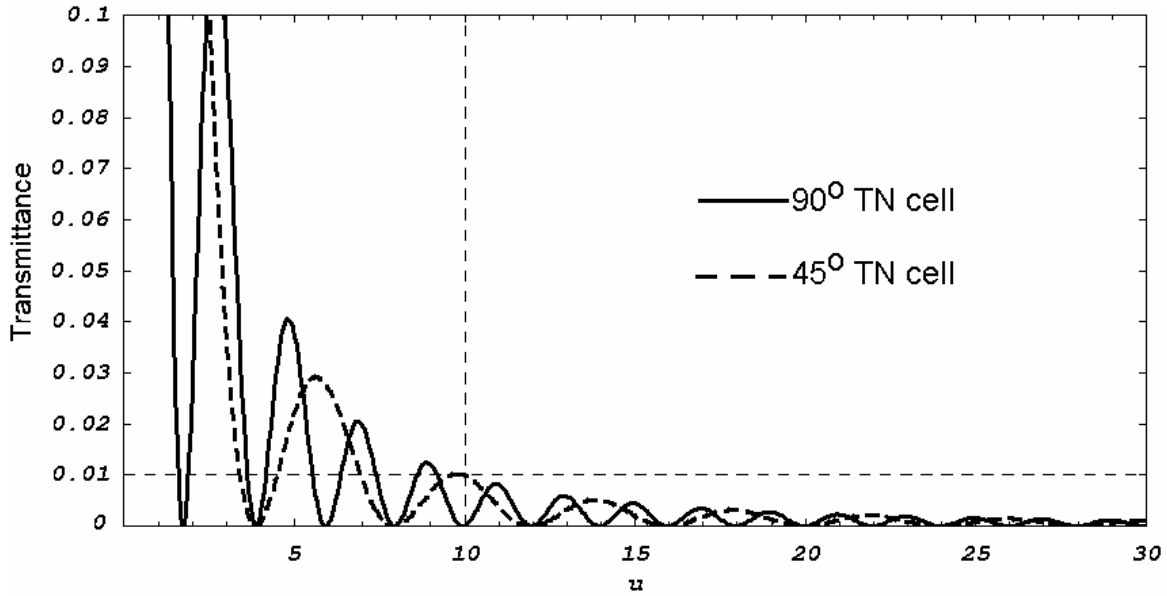


Fig. 1. Transmittance T vs. the Mauguin parameter u calculated with Eq.(1) for 90° (solid line) and 45° (dashed line) TN cells.

Figure 1 shows the transmittance T vs. the Mauguin parameter u calculated using Eq.(1) for 90° and 45° TN cells. As expected, for a large u that corresponds to the Mauguin regime, the transmittance decreases nonmonotonously, through the series of decreasing maxima and zeros. The amplitudes of maxima depend only on u whereas the positions of maxima and zeros depend on both u and Θ . One can consider that the cell performs in the Mauguin regime when $T < 1\%$ and, therefore, when $u \geq 10$ for any twist angle Θ . This condition shows that to design a 90° achromatic rotator for $\lambda \leq 2 \mu m$ with a nematic material of typical birefringence $\Delta n = 0.22$, one should use a TN cell of a rather large thickness, at least $45 \mu m$. Such a thick cell would show extremely slow dynamics [17], as the relaxation time of TN cell when the field is switched off is determined by:

$$\tau_{OFF} \approx \frac{\gamma_1 d^2}{\pi^2 K_{eff}} \sim 1 s, \quad (2)$$

where $\gamma_1 \sim 0.1 kg \cdot m^{-1} \cdot s^{-1}$ is the rotational viscosity and $K_{eff} \sim 10^{-11} N$ is the effective elastic constant of a typical nematic material [6].

To resolve the contradictory requirements of a short response time and a chromatic compensation of a switched TN cell, several multi-element approaches have been explored. The TN cell may be replaced by a linear polarization rotator containing two or more switchable LC cells. For example, two identical half-wave plates were used for the achromatic rotation of the linearly polarized light in the range (450 – 700 nm) [1, 2]. The second half-wave plate was oriented to double the polarization rotation while suppressing the elliptic polarization induced by the first one. In the three element design, the ferroelectric LC half-wave switchable plate [7] or a thin 90° TN cell [8, 9] were placed between two passive birefringent plates; the resulting transmittance is high $T \geq 0.98$ in the visible range (400 – 700 nm). The achromatic polarization switch with a nematic cell sandwiched between two identical 135° TN cells was designed and showed good performance for visible or near infrared spectral ranges [10, 11]. The multi-element optical design, however, imposes strict requirements for the refractive indices matching and requires antireflection layers to diminish the interference of reflected and transmitted beams.

A thick TN cell ($d \approx 40 \mu m$) was tested as a polarization switch of infrared radiation at $10.6 \mu m$ [17]. The switch off time of the thick TN cell was about 0.5 s in agreement with Eq.(2).

In this work, we propose polarization rotators based on TN cells filled with the so-called dual-frequency nematics. The distinctive feature of a dual-frequency nematic is a frequency dependent dielectric anisotropy $\Delta \epsilon(f) = \epsilon_{||}(f) - \epsilon_{\perp}(f)$

which is positive below some critical frequency f_c and negative at $f > f_c$, here $\epsilon_{||}$ and ϵ_{\perp} are the dielectric permittivities referred to the director \mathbf{n} . The driving voltage aligns the director parallel to the field when $f < f_c$ and perpendicular to it when $f > f_c$. The dual-frequency nematic allows one to reduce the relaxation time because the direct and reversed transitions between the twisted and homeotropic states are controlled by the driving voltage of proper amplitude and frequency.

For a TN cell with planar alignment (the director \mathbf{n} is parallel to the bounding substrates), the switching time of the polar angle for director reorientation towards the homeotropic state (parallel to the applied field of low frequency f_l) is:

$$\tau_l \approx \frac{\gamma_1 d^2}{\epsilon_o \Delta\epsilon(f_l) U^2 - \pi^2 K_{eff}}, \quad (3)$$

where ϵ_o is the free-space permittivity and U is the RMS applied voltage. The switching time of polar angle for the director reorientation from normal back to the TN state (perpendicular to the applied field with high frequency f_h) is:

$$\tau_h \approx \frac{\gamma_1 d^2}{\epsilon_o |\Delta\epsilon(f_h)| U^2 + \pi^2 K_{eff}}. \quad (4)$$

Assuming that $\Delta\epsilon(f_l) \approx -\Delta\epsilon(f_h) \approx 3$, one can make both τ_l and τ_h two orders of magnitude shorter than τ_{OFF} in Eq.(2) by applying $U \approx 30 V$.

Furthermore, if the original director orientation is not planar, but strongly tilted with respect to the boundary plates, $\alpha \approx \pi/4$, both τ_l and τ_h are short, as described by the formula [12]:

$$\tau_{l,h} \approx \frac{\gamma_1 d^2}{\epsilon_o |\Delta\epsilon(f_{l,h})| U^2 + 2K_{eff}}, \quad (5)$$

We explore two approaches to design a switchable broadband polarization rotator based on dual-frequency TN cells, either (2.1) one 90° TN cell or (2.2) two 45° TN cells with opposite handedness.

2.1. 90° TN cell

Equations (3-5) show that fast switching dual-frequency TN cells allows one to employ the simplest switchable broadband polarization rotator, namely, 90° TN cell working in the Mauguin regime. The polarizer is parallel to the director at the entrance plane of the TN cell. The transmitted light may have one of the two orthogonal polarizations: parallel to director at the exit plane if the director remains in the twisted state or perpendicular to director at the exit plane if the applied voltage transfers the director into homeotropic state. The 90° TN cell does not require complete reorientation into the homeotropic state because if the bulk region in the middle of the cell is in homeotropic state, the remaining distorted regions near the surfaces do not change the state of polarization. The performance quality of the achromatic rotator is determined by how small is the maximum intensity of the unwanted polarization in the required range $\lambda_{\min} \leq \lambda \leq \lambda_{\max}$ is. This intensity is determined by the largest T_{\max} for $u \geq u_{\min}$ in Fig.1, where $u_{\min} = \pi d \Delta n(\lambda_{\max}) / \lambda_{\max} \Theta$. For a rotator with an *a priori* defined quality $T < T_{\max}$, the formula for u_{\min} above defines the minimum cell thickness:

$$d_{\min} = \frac{u_{\min}(T_{\max}, \Theta) \lambda_{\max} \Theta}{\pi \Delta n(\lambda_{\max})} \quad (6)$$

Obviously, the thicker cells are more desirable. However, in addition to the longer switching time, the thick cells might pose another problem, related to the backflow effect, i.e. material flows triggered by the director reorientation. To mitigate the backflow effect, we used a polymer stabilization technique [18, 19]

2.2. Two 45° TN cells

The second approach for achromatic polarization rotator is a pair of 45° TN cells arranged as shown in Fig.2. A horizontally polarized light beam is passing through the right-handed (TN1) and left-handed (TN2) TN cells. The easy axes at the incident and output substrates of the cells are shown by arrows in Fig.2. When the voltage is applied only to TN1, to switch it into the homeotropic state, the incident polarization is rotated by 45° counterclockwise by TN2, which is in the “off” state (no voltage applied). If TN2 is switched “on” and TN1 is “off”, then the incident polarization is rotated by 45° clockwise. As a result, depending on states of TN1 and TN2, the output light would have two mutually orthogonal linear states of polarization.

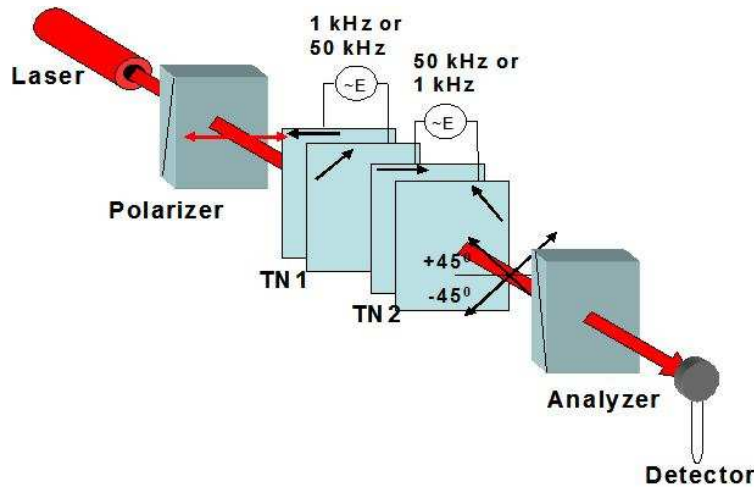


Fig.2. Polarization rotator scheme utilizing two 45° TN cells with opposite handedness.

The main advantage of this approach is that the 45° TN cells can be approximately 2 times thinner than 90° TN cell because $d_{\min} \propto \Theta$, see Eq.(6). Decreasing the thickness by a factor of 2 makes the cell faster by a factor of 4, as $\tau \propto d^2$, Eq.(3-5). However, a drawback of the approach is in the increased number of reflective surfaces (two cells instead of one); the problem can be mitigated by using one common glass plate for two cells, with conducting electrodes at both sides. Second, the incomplete reorientation of the director near the boundaries of the cell in the homeotropic state might transform the incident linear polarization into elliptical. This unwanted transformation occurs because the director alignment is at the angle of 45° with respect to the linear polarization of propagating light.

3. CELL PREPARATION

3.1. 90° TN cell

We use polymer-stabilized dual-frequency TN cells with the planar alignment on the glass substrates and the dual-frequency nematic mixture MLC2048 with $f_c = 12.9 \text{ kHz}$, $\Delta\epsilon = 3.2$ at $f_l = 1 \text{ kHz}$ and $\Delta\epsilon = -3.1$ at $f_h = 50 \text{ kHz}$ (all data for the room temperature) [13]. The planar alignment layers were prepared in a standard way by spin coating, baking, and rubbing the polyimide PI2555 (HD Microsystems L.L.C.) over the conducting indium tin oxide (ITO) electrodes of the glass substrates. The rubbed substrates were assembled in an orthogonal fashion. The cell gap of 45 μm was fixed by polyester films. The cell was filled with a mixture of MLC2048, a right chiral dopant R1011 (concentration 0.01% by weight), and a reactive mesogen RM257 (2%), all purchased from EM Industries. The small amount of R1011 was added to avoid degeneracy between the right and left twists and to assure a homogeneous right

handed twist. The helical twisting power $HTP \cong 28.4 \mu\text{m}^{-1}$ of R1011 in MLC2048 was measured in the lab. Note that an excessive amount of chiral dopant might spoil optical performance of the cell in the homeotropic state by inducing a strong twist in the regions near the substrates.

The reactive mesogen RM257 was used to diminish the back-flow effects by developing a polymer network inside the cell. The filled cell was cured under ultraviolet light of intensity 40 mW/cm^2 for 30 minutes at room temperature. The polymer chains of mesogenic monomer grow along the director [20]. In order to form a polymer network connected to both substrates, we polymerized the mixture in the presence of the low-frequency voltage ($\approx 30 \text{ V}$) that kept the director in the homeotropic state. The connected polymer network mitigated the backflow effect and reduced the light scattering as compared to the polymer network created in the planar state. Note that a useful side effect of this polymerization approach was that in the field-off state, the director in the bulk of the cell was somewhat tilted away from the planar orientation, thus increasing the dielectric torque and eliminating the threshold of reorientation when the field was applied.

3.2. 45° TN cells

We prepared two 45° TN cells with opposite handedness filled with the dual-frequency material MLC-2048, using ITO glass substrates with obliquely deposited SiO that provides a high pretilt alignment (about 45° for MLC 2048) of the director. A high pretilt angle together with dual-frequency feature of the LC material and overdriving technique allows one to significantly reduce the cell switching time [12]. Using Eq.(6) and optical characteristics of the MLC-2048, one can see that a 45° TN cell of thickness $20 \mu\text{m}$, would provide efficient rotation ($T_{\text{max}} < 0.03$) of the polarization of incident light by 45° in a wide spectral range ($0.5 - 2.7 \mu\text{m}$).

No chiral dopants were used for preparation of the 45° TN cells.

4. EXPERIMENTAL RESULTS

4.1. Thick 90° TN cell

We tested experimentally the switching performance of $45 \mu\text{m}$ thick TN cell in the so-called normally white mode [16], with the TN cell sandwiched between a pair of crossed polarizers, Fig.3 (a). The TN cell was oriented to have the incident light polarized along the rubbing direction at the plate of incidence. Figure 3 (b,c) shows how the transmitted light intensity (top run) is affected by the applied voltage at different frequencies (bottom run) that switches the state of polarization by 90 degrees. Part (b) shows the intermediate states of polarization, while part (c) shows the abrupt changes of polarization by 90 degrees. In the field free state, the TN cell shows an intermediate level of the transmission (because of some tilt in the middle of the cell produced during the UV-polymerization), Fig.3 (b). The low-frequency voltage establishes the homeotropic state (zero transmittance in Fig. (b,c)) and the high frequency voltage establishes the TN state with the director perpendicular to the field and thus parallel to the bounding plates (maximum transmittance in Fig. 3(b,c)).

To speed up the switching process, we used short pulses of high amplitude at both driving frequencies followed by lower holding voltages [12]. Typically, the short pulses were of RMS amplitude of 50V and holding voltage of 16 V at 1 kHz and 20 V at 50 kHz. Figure 3 (c) demonstrates the oscilloscope pictures of fast switching between the twisted and homeotropic states. The response time was 10 ms for both direct and reverse transitions between the homeotropic and twisted states.

To determine the transmission spectra of the rotated linearly polarized light, we placed the polymer-stabilized $45 \mu\text{m}$ thick TN cell between parallel polarizers (normally black mode of a TN cell [16]) in the sample compartment of a Spectrum One NTS PerkinElmer infrared spectrometer. Figure 4 shows the transmission spectra of the TN cell in the homeotropic and twisted states versus the wavelength (solid line) in comparison with the calculated transmission (dashed line) of the twisted state calculated using Eq.(1) and the data on optical dispersion of MLC 2048 [21].

The transmission of the TN cell was $T \geq 0.9$ in the homeotropic state and $T \leq 0.02$ for the TN state, in the broad spectral range ($0.4 - 2.7 \mu\text{m}$), Fig.4. Note that the performance of the TN cell was not optimized as we did not employ antireflection layers of any kind.

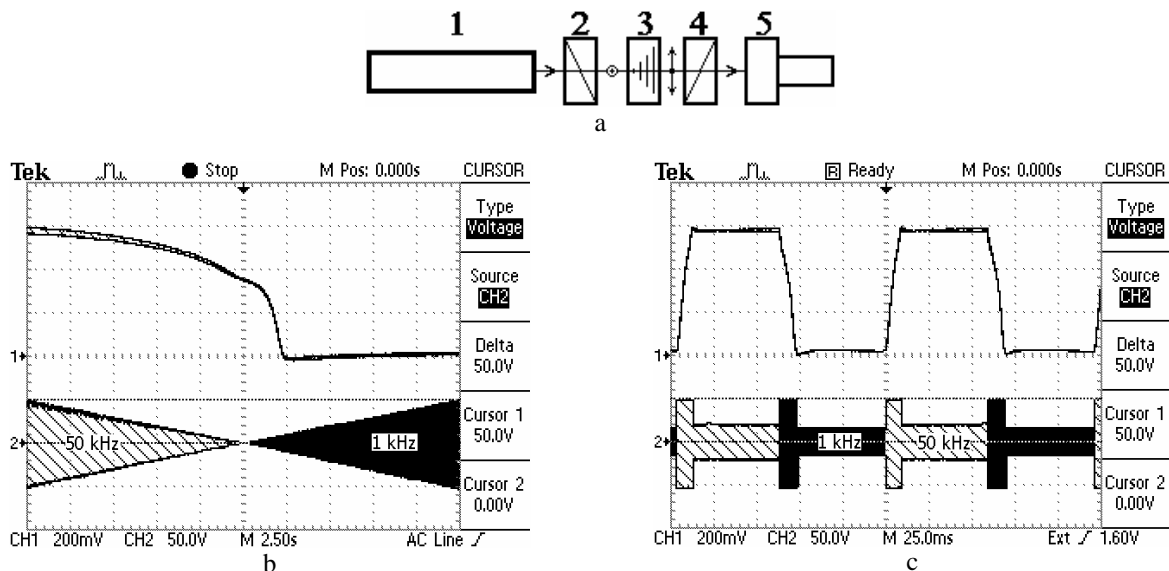


Fig.3. a) Optical setup: (1) diode laser with $\lambda \approx 1.55\mu\text{m}$, (2) polarizer prism, (3) TN cell, (4) analyzer prism, and (5) photodiode; b) transmitted light intensity (top trace) vs. slowly changing sinusoidal voltage (bottom trace that shows envelope of the sinusoid) applied at two different frequencies: 50 kHz (left part of the bottom trace) and 1 kHz (right part), the time scale is 2.5 s/square; c) fast switching of the same TN cell by a sequence of Special Short Pulses ($U_{1\text{kHz}}=U_{50\text{kHz}}=50\text{V}$) and holding voltages ($U_{1\text{kHz}}=16\text{V}$, $U_{50\text{kHz}}=20\text{V}$), time scales are 25 ms/square.

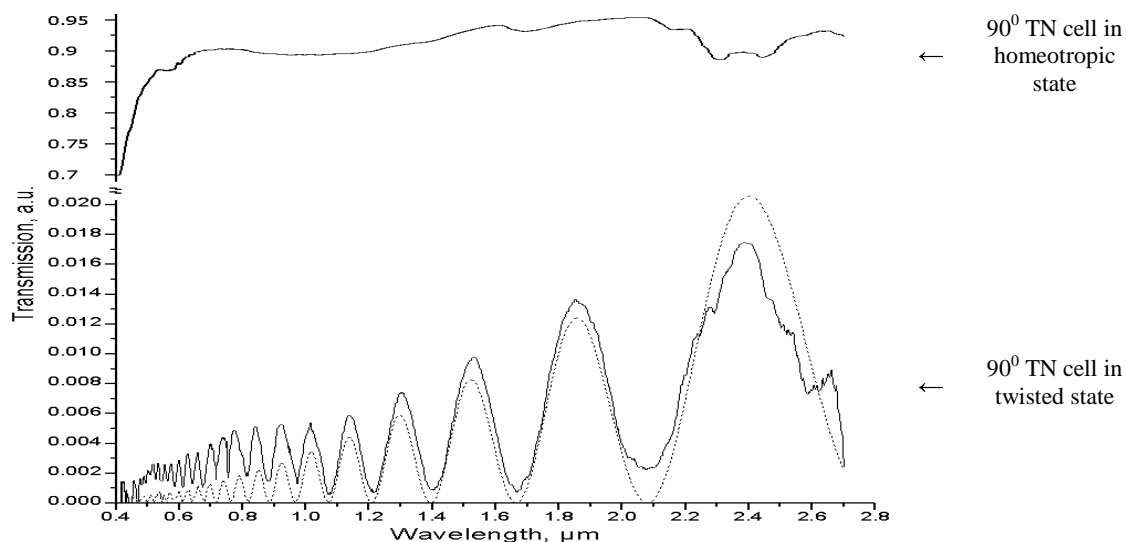


Fig.4. Transmission spectra of the polymer-stabilized 90° TN cell of thickness $d \approx 45\mu\text{m}$ placed between two parallel polarizers vs. wavelength (solid line) and approximation accordingly to (2) (dashed line).

4.2. Pair of 45° TN cells

Figure 5 shows the transmission of linearly polarized light through the pair of electrically controlled 45° TN cells (arranged as in Fig.2) at $\lambda = 1.55\mu\text{m}$. The two cells are of opposite handedness. Each cell is of thickness $20\mu\text{m}$ and has a high-pretilt alignment set by SiO deposition. To switch the cells between the homeotropic and planar twisted state we applied the overdriving technique with high-amplitude pulses and holding voltages at frequencies 1 and 50 kHz. The analyzer was parallel to the output easy axis of the second TN cell. The optical signal is changing from maximum to minimum as the linear polarization of light is switched between the two orthogonal orientations. The switching time of both TN cells is about 2 ms, which is two orders of magnitude faster than for the $20\mu\text{m}$ thick cell switched in the

conventional mode, according to Eq.(3). The fast response, however, is accompanied by a slow drift in the transmitted intensity (less than 5%) when the cell is switched to the homeotropic state. A similar effect was observed in the 90° TN cell with no polymer stabilization and might be related to the backflow effect and thus might be mitigated by the polymer stabilization.

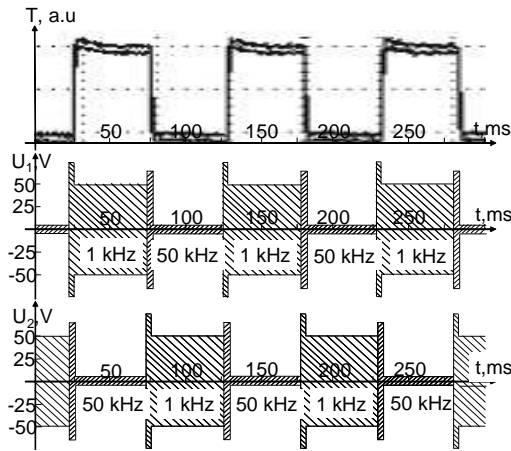


Fig.5. Switching of the pair of 45° TN cells at $\lambda = 1.55 \mu\text{m}$ (upper trace) performed by the sequence of high amplitude short pulses ($U_{1\text{kHz}}=74\text{V}$, $U_{50\text{kHz}}=66\text{V}$) and holding voltages ($U_{1\text{kHz}}=50\text{V}$, $U_{50\text{kHz}}=5\text{V}$) at two frequencies 1kHz and 50kHz. Driving voltage U_1 (middle trace) applied to TN1; U_2 (bottom trace) applied to TN2. The response time of each cell is about 2 ms.

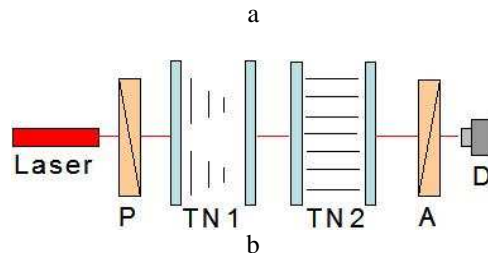
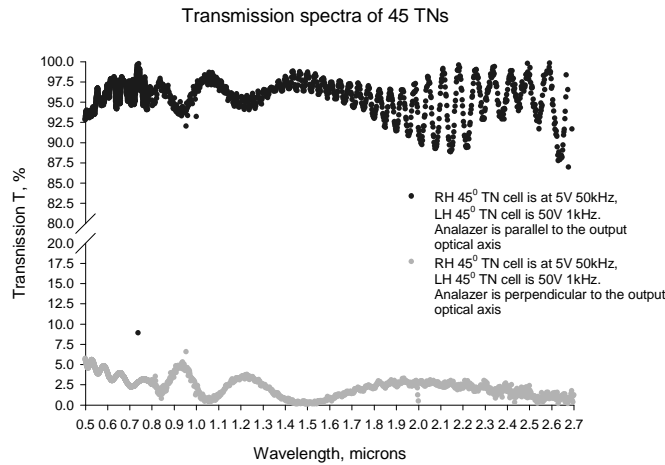


Fig.6. Transmission spectra of the pair of 45° TNs with opposite handedness (a); TN cells arrangement and voltages applied during measurement of transmission spectra (b).

In Fig.6a we show the normalized transmission spectra of the pair of 45° TNs. During the transmission spectra measurements the TN1 was in the planar state ($U_{50\text{kHz}}=5\text{V}$) while the TN2 was in the homeotropic state ($U_{1\text{kHz}}=50\text{V}$) as shown in Fig.6b. The analyzer was oriented parallel to the output easy axis of the TN1 (upper curve, Fig.6a) or perpendicular to it (bottom curve, Fig.6a). The transmission spectra for the opposite case (TN1 homeotropic and TN2

planar) are similar. The optical transmission of $T > 90\%$ was observed in the wide spectral range $0.5 - 2.7 \mu\text{m}$. In the visible part of the spectrum, the intensity of the unwanted light polarization is higher than for the infrared region (Fig.6a), which is in apparent contradiction to Eq.(1). This behavior of the transmitted signal is most probably caused by the residual director distortions near the surfaces that can modify the incident linear polarization into the elliptical one and thus lead to the leakage of undesired polarization of light. This leakage is more pronounced for shorter wavelengths. It is not significant in 90° TNs as the director orientations at the opposite substrates are mutually perpendicular. In 45° TNs, the parasitic effect can be mitigated by further optimization of cell parameters such as the twist angle and adjustments of mutual orientation of the cells.

The optical signal experiences some additional oscillations in the infrared part of the spectra (upper curve, Fig.6a), which may be caused by Fresnel reflections at the interfaces air/glass, glass/ITO, ITO/LC; the issue can be addressed by using antireflection coatings and conductive electrodes more transparent in the infrared part of the spectrum.

5. CONCLUSIONS

We explored two approaches to design the achromatic linear polarization switch for a broad spectral range from visible to near-infrared. The achromatic linear polarization switch based on the polymer-stabilized dual-frequency 90° TN cell with a $45 \mu\text{m}$ thickness showed a response time of 10 ms and optical transmission of $T \geq 0.9$ in the broad spectral range from 0.4 to $2.7 \mu\text{m}$. We further improved switching performance by replacing the 90° TN cell with two 45° TN cells, that allowed us to obtain a faster response time, about 2 ms, while preserving a relatively high level of optical transmission at $T \geq 0.9$.

We acknowledge the partial support of the Air Force Research Laboratory through the KSU subcontract to grant F33615-00-C-1683 and NSF grants DMR-0504516 and DMS -0456221; we thank P. Bos and B. Winker for stimulating and useful discussions of the issues related to this project.

REFERENCES

1. G. Anderson, I. Dahl, L. Komitov, S.T. Lagerwall, K. Skarp, and B. Stebler, *J.Appl. Phys.* **66**, 4983 (1989).
2. J.E. Stockley, G.D. Sharp, D. Doroski, and K.M. Johnson, *Opt. Lett.* **19**, 758 (1994).
3. M. Schadt and W. Helfrich, *Appl.Phys.Lett.* **18**, 127 (1971).
4. M.C. Mauguin, *Bull. Soc. Fr. Mineral* **34**, 71 (1911).
5. C. Gooch and H. Tarry, *J. Phys. D* **8**, 1575 (1975).
6. L.M. Blinov and V.G. Chigrinov, *Electrooptics Effects in Liquid Crystal Materials* (Springer, New York, 1994), pp.133-234.
7. P. Hariharan and P.E. Ciddor, *Opt. Eng.* **36**, 952 (1997).
8. Z. Zhuang, Y.J. Kim, and J.S. Patel, *Appl. Phys. Lett.* **76**, 3995 (2000).
9. Q. Wang, T.X. Wu, X. Zhu, and S.T. Wu, *Liquid Crystals* **00**, 1 (2004).
10. M.D. Lavrentovich, T.A. Sergan, J.R. Kelly, *Opt. Lett.* **29**, 1411 (2004),
11. J.R. Kelly, H.J. Yuan, and Q. Li, U.S. patent appl. COAD-003/01US, 10/035,804 (2001).
12. A.B. Golovin, S.V. Shianovskii, and O.D. Lavrentovich, *Appl. Phys. Lett.* **83**, 3864 (2003).
13. Y. Yin, M. Gu, A.B. Golovin, S.V. Shianovskii, and O.D. Lavrentovich, *Mol. Cryst. Liq. Cryst.* **421**, 133 (2004).
14. Y. Yin, S.V. Shianovskii, A.B. Golovin, and O.D. Lavrentovich, *Phys. Rev. Lett.* **95**, 087801 (2005).
15. Hl. de Vries, *Acta Cryst.* **4**, 219 (1951).
16. P. Yeh and C. Gu, *Optics of Liquid Crystal Displays* (J.Wiley&Sons Inc, New York, 1999), pp. 161-193.
17. S. Brugioni and R. Meucci, *Opt. Comm.* **216**, 453 (2003).
18. P.J. Bos, J.A. Rahman, and J.W. Doane, *SID'93 Tech.Digest*, 877 (1993).
19. S.H. Kim and L.C. Chien, *Jpn. J. of Appl. Phys.* **43**, 7643 (2004).
20. G.A. Held, L.L. Kosbar, I. Dierking, A.C. Lowe, G. Grinstein, V. Lee, and R.D. Miller, *Phys. Rev. Lett.* **79**, 3443 (1997).
21. We use Cauchy dispersion formulas $n_o(\lambda) \approx 1.47 + 9.73 \cdot 10^{-3} \cdot \lambda^{-2} - 2.56 \cdot 10^{-4} \cdot \lambda^{-4}$ and $n_e(\lambda) \approx 1.67 + 5.46 \cdot 10^{-3} \cdot \lambda^{-2} + 4.24 \cdot 10^{-3} \cdot \lambda^{-4}$ for MLC2048, where λ is measured in microns.